VOL. 11, NO. 15, AUGUST 2016 ISSN 1819-6608
ARPN Journal of Engineering and Applied Sciences

www.arpnjournals.com

PERFORMANCE ANALYSIS OF A VERTICAL WELL WITH A FINITE-CONDUCTIVITY FRACTURE IN GAS COMPOSITE RESERVOIRS

Yu Long Zhao[1], Freddy Humberto Escobar[2], Claudia Marcela Hernandez[2] and Chao Ping Zhang[3]
[1]State Key Laboratory of Oil and Gas Reservoir Geology and Exploitation, Southwest Petroleum University, Chengdu, Sichuan, P.R. China
[2]Universidad Sur colombiana/CENIGAA, Avenida Pastrana, Neiva, Huila, Colombia
[3]Northeast Sichuan Gas Production Branch of Southwest China Oil and Gas Field, Petro China, P.R. China
E-Mail: fescobar@usco.edu.co

ABSTRACT

It is well known that hydraulic fracturing can efficiently be applied to develop both low permeability and unconventional gas reservoir. Sometimes, the formations cannot be fully fractured and, then, the resulting fracture does not end up with infinite conductivity. Besides, for either tight or unconventional gas reservoir, a fracture network will be developed around the well during the fracturing process. This paper presents a semi-analytical model governing fluid flow in porous material for a finite-conductivity-fractured well in a composite gas reservoir, considering the fractures as either partially or fully penetrated. By nature, a fracture-network system around the well is always induced in tight gas formations, then, a composite model with inner dual-porosity to describe stimulated reservoir volume is established. Solutions for both constant-production rate and constant-bottom hole pressure are obtained by using the point-source function and the Laplace transformation techniques which are used along with the Stehfest algorithm to obtain the numerical inversion of the pressure and rate variables. The pressure-time and rate-time behaviours are then analyzed by careful observation to both transient-pressure and the rate-decline type curves. The models and type curves introduced in this work possess both theoretical and practical valuable application in the field of well test interpretation for the system under consideration.

Keywords: fracture conductivity, gas reservoirs, well testing, rate decline, composite systems.

1. INTRODUCTION

Hydraulic fracturing has been an efficient tool to develop low-permeability reservoir, such as tight hydrocarbon formations and coal seam gas. Besides, gas shale formation only can be produced by means of hydraulically-fractured wells. In the mentioned situations, well stimulation by fracturing is only conducted once in the life of the well and greatly enhances fluid removal and well productivity. Hydraulic fracturing occurs when the effective stress has overcome sufficiently by an increase in the fluid pressure within the rock, so that the minimum principle stress becomes tensile and exceeds the tensile strength of the material. Fractures formed under this procedure will mainly be oriented in the plane perpendicular to the minimum principal stress, and for this reason, induced hydraulic fractures in wellbores are sometimes used to determine the orientation of stresses, Fjaer (2008).

From experience and rock mechanics analyses, it has been found that the fracture height is often determined by the existence and position of barriers above and below the fracturing zone. So a partially-penetrated fracture will be formed when the reservoir has some hard limited scale among interlayer's or barriers. During the fracturing process, the fracturing high-pressure fluid pumped down into the formation always flows into the porous medium in which a damage zone around the well may be present. The damage zone with the outer zone always can be treated as a radial composite system. Moreover, the fractured-radial-composite system can also occur naturally or may be artificially created. Aquifers with two different perm abilities, oil and water regions or gas and oil regions with different reservoir properties are typical examples of naturally occurring. Other examples of composite systems include secondary and tertiary recovery projects in oil reservoirs and produced water reinjection gas reservoirs.

Since transient pressure and rate decline analysis methods are of important application to hydrocarbon industry so engineers can recognize the formation and fracturing characteristics, many models have been proposed to describe the fluid seepage flow theory from the formation to the well and developed many detailed semi-analytical solutions for both finite and infinite-fracture conductivity as described by Prats (1961), Gringarten, Ramey, Raghavan (1974a, 1974b), Cinco-Ley and Samaniego (1981), Cinco-Ley, Samaniego and Dominguez (1978), Hanley and Bandyopadhyay (1979), Ahmed (1982) and Mohammed (1993).

Prats (1961) analyzed the performance of a finite-conductivity vertical fractured-well performance. Cinco-Ley and Samaniego (1977) investigated the effects of wellbore storage and fracture damage on the well performance and indicated that these effects should be taken into account in well test analysis. Cinco-Ley, Samaniego and Rodriguez (1989) presented a semi-analytical model and type curves for the analysis of pressure data of wells intersected by finite- conductivity vertical fractures in infinite slab reservoirs. Hanley and Bandyopadhyay (1979) presented a simple semi-analytical model for a well in a square reservoir with a uniform flux fracture fully penetrating the formation in the horizontal direction. Ahmed (1982) presented a detailed study on all the available specialized plots used to analyze various types of hydraulic fractures and formation flow regimes.

Cinco-Ley, Samaniego and Rodriguez (1989) observed a flow regime "pseudo-linear" to distinguish it from the real linear flow characterizing the infinite-conductivity fracture. Mohammed (1993) developed a mathematical model to analyze the pressure behavior of a fractured well located in a multilayered reservoir. Mohammed and Kassem (1997) presented a mathematical model for describing the pressure behavior of a vertical-fractured well located in a stratified, bounded, square reservoir.

For fractured wells in composite reservoir, Chu and Shank (1993) presented a mathematical model for a vertical-fractured well having either finite conductivity or uniform flux in a composite system. Chen and Raghavan (1995) developed a model for a fractured well producing in a composite reservoir. They also addressed some computational issues during the computation of the products $I_n(x)\cdot K_n(x)$. Feng, Luo and Cheng (2009) proposed a seepage flow model for fractured heterogeneous composite reservoirs using equivalent flowing resistance method. However, a few of them have taken into account the effect of wellbore storage and skin factor in their modeling. Besides, no consideration of partial penetrating fractures has been reported by these researchers. Zhao (2011) derived a continuous point-source solution in radial-composite gas reservoir and, later, the transient pressure of fully and partially fractured well with finite-conductivity in a radial composite reservoir is analyzed Zhao *et al*. (2013).

As mentioned above, the various methods and models presented in the literature mostly aimed at the well with infinite or finite conductivity in homogeneous reservoir, and only a few of them reported the pressure and rate transient performance of partially fractured wells with finite conductivity in composite reservoir as well as the multi-porosity media composite models. The main objective of this paper is to fill this gap and to investigate the pressure behavior and rate decline performance of a radial-composite gas reservoir containing either a partially or fully penetrating hydraulic fracture with finite conductivity. The solution is achieved by combining the continuous point source with the fracture flow model, and then the semi-analytical solution is obtained by the Laplace transformation method and boundary element integral method. Finally, the performance of a new composite model with inner dual porosity to describe the fracture network (stimulated reservoir volume) created by massive hydraulic fracturing is analyzed. This mathematical model was used by Escobar, Zhao and Zhang (2014) to provide an interpretation solution using characteristic points and lines found on the pseudopressure and pesudopressure derivative plot.

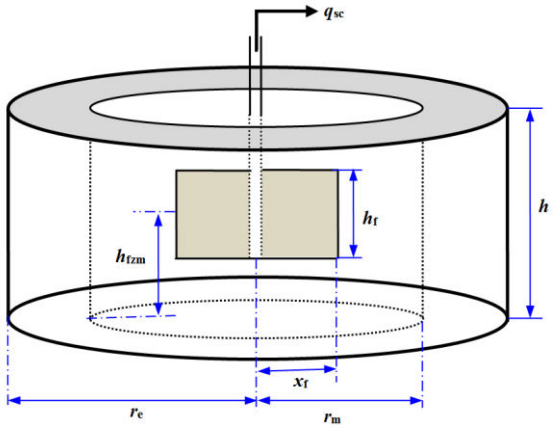

Figure-1. Schematic representation of a finite-conductivity fractured well in bi-zonal gas reservoir.

2. MATHEMATICAL MODEL

2.1 Reservoir flow model

The transient pressure behavior in the reservoir can be studied by considering the fracture as a plane source of height, h_f, length $2x_f$ and flux density $q_f(x,t)$, see Figure-1. According to the continuous point-source function of the inner region in bi-zonal gas reservoir as presented by Zhao (2011) the solution for the partially penetrating fractured well can be easily obtained by integrating the continuous source function obtained before with respect to x_{wD} and z_{wD} over the penetrating interval, which is:

$$\Delta\bar{\psi}_{1D}(x_D,y_D,s)=\frac{1}{2M_{12}}\int_{-1}^{1}q_{fD}(\alpha,s)\left\{\begin{array}{l}K_0\left(\sqrt{(x_D-\alpha)^2+y_D^2}\sqrt{s\eta_{rD}}\right)+\\ D_0\cdot I_0\left(\sqrt{(x_D-\alpha)^2+y_D^2}\sqrt{s\eta_{rD}}\right)+\frac{4}{\pi h_{fD}}\times\\ \sum_{n=1}^{+\infty}\left[\begin{array}{l}K_0\left(\sqrt{(x_D-\alpha)^2+y_D^2}\sqrt{s_n}\right)\\ +D_n\cdot I_0\left(\sqrt{(x_D-\alpha)^2+y_D^2}\sqrt{s_n}\right)\end{array}\right]\\ \cos(n\pi z_D)\cdot\cos(n\pi h_{fzmD})\cdot\sin(n\pi\frac{h_{fD}}{2})\end{array}\right\}d\alpha \quad (1)$$

where,

$$D_n=\frac{\Omega_n}{\chi_n}\quad(n=0,1,2,\cdots) \quad (2)$$

$$\Omega_n=K_0\left(r_{mD}\sqrt{s_n}\right)\left[K_0'\left(r_{mD}\sqrt{s_n}\right)+A_n\right]-M_{12}K_0'\left(r_{mD}\sqrt{s_n}\right)\left[K_0\left(r_{mD}\sqrt{s_n}\right)+B_n\right] \quad (3)$$

$$\chi_n=M_{12}I_0'\left(r_{mD}\sqrt{s_n}\right)\left[K_0\left(r_{mD}\sqrt{s_n}\right)+B_n\right]-I_0\left(r_{mD}\sqrt{s_n}\right)\left[K_0'\left(r_{mD}\sqrt{s_n}\right)+A_n\right] \quad (4)$$

For the lateral infinite boundary:

$$A_n=B_n=0 \quad (5)$$

For lateral closed boundary:

$$A_n = I_0'\left(r_{mD}\sqrt{\tilde{s}_n}\right)\frac{K_1\left(r_{eD}\sqrt{\tilde{s}_n}\right)}{I_1\left(r_{eD}\sqrt{\tilde{s}_n}\right)}, B_n = I_0\left(r_{mD}\sqrt{\tilde{s}_n}\right)\frac{K_1\left(r_{eD}\sqrt{\tilde{s}_n}\right)}{I_1\left(r_{eD}\sqrt{\tilde{s}_n}\right)} \quad (6)$$

For lateral constant-pressure boundary:

$$A_n = -I_0'\left(r_{mD}\sqrt{\tilde{s}_n}\right)\frac{K_0\left(r_{eD}\sqrt{\tilde{s}_n}\right)}{I_0\left(r_{eD}\sqrt{\tilde{s}_n}\right)} B_n = -I_0\left(r_{mD}\sqrt{\tilde{s}_n}\right)\frac{K_0\left(r_{eD}\sqrt{\tilde{s}_n}\right)}{I_0\left(r_{eD}\sqrt{\tilde{s}_n}\right)} \quad (7)$$

$$s_n = s\eta_{rD} + \frac{n^2\pi^2}{h_D^2} \quad 7(a)$$

$$\tilde{s}_n = s + \frac{n^2\pi^2}{h_D^2} \quad (8)$$

Dimensionless parameters

Agarwal (1979) introduced a pseudotime function to account for the time dependence of gas viscosity and total system compressibility as follows:

$$t_a = \int_{t_o}^{t}\frac{1}{\mu(t)c_g(t)}dt \quad (9)$$

For compressible fluids, the pseudopressure, $\psi(p)$, introduced by Agarwal (1979) is given by:

$$\psi(p) = 2\int_0^p \frac{p}{\mu(p)Z(p)}dp \quad (10)$$

Define the dimensionless quantities as follows:

$$t_D = \frac{3.6k_{r2}t_a}{\phi_1 x_f^2} \quad (11)$$

$$h_{fD} = \frac{h_f}{h} \quad (12)$$

$$h_{fzmD} = \frac{h_{fzm}}{h} \quad (13)$$

$$z_D = \frac{z}{h} \quad (14)$$

$$r_{mD} = \frac{r_m}{x_f} \quad (15)$$

$$M_{12} = \frac{k_{r1}}{k_{r2}} \quad (16)$$

$$\eta_{rD} = \frac{k_{r2}\phi_1}{k_{r1}\phi_2} \quad (17)$$

$$h_D = \frac{h}{x_f}\sqrt{\frac{k_{r1}}{k_{z1}}} \quad (18)$$

$$h_D = \sqrt{\frac{k_{r1}k_{z2}}{k_{r2}k_{z1}}}h_D \quad (19)$$

$$\psi_D = \frac{k_{r2}hT_{sc}}{3.684\times10^{-3}q_{sc}p_{sc}T}\Delta\psi \quad (20)$$

$$q_{fD}(x_D, t_D) = \frac{2x_f q_f(x_D, t_D)}{q_{sc}} \quad (21)$$

2.2 Fracture flow model

The fracture is considered as a homogeneous, finite, slab, porous medium of height, h_f, length $2x_f$ and width, w_f, fluid enters the fracture at a rate $q_f(x, t)$ per unit of fracture length, and flow across the edge of this porous medium is negligible because the fracture width is very small compared to the fracture length. The assumptions allow us to consider a linear flow regime in the fracture and permits simulation of well production by a uniform-flux plane source of *hf* and *w*, located at the wellbore axis.

Define the dimensionless fracture conductivity, C_{fD}, and the dimensionless fracture width, w_{fD} as follows:

$$C_{fD} = \frac{w_f k_f}{k_{r2}x_f} \quad (22)$$

$$w_{fD} = \frac{w_f}{x_f} \quad (23)$$

According to the researches of previous Cinco-Ley *et al.* (1978, 1989), the dimensionless model of the fluid flow in fracture system becomes:

$$\frac{\partial^2\bar{\psi}_{fD}}{\partial x_D^2} + \frac{2M_{12}}{C_{fD}}\left.\frac{\partial\bar{\psi}_{1D}}{\partial y_D}\right|_{y_D=\frac{w_{fD}}{2}} = 0, 0 < x_D < 1 \quad (24)$$

$$\left.\frac{\partial\bar{\psi}_{fD}}{\partial x_D}\right|_{x_D=0} = -\frac{\pi}{sC_{fD}h_{fD}} \quad (25)$$

$$\bar{q}_{fD}(x_D, s) = -\frac{2h_{fD}M_{12}}{\pi}\left.\frac{\partial\bar{\psi}_{1D}}{\partial y_D}\right|_{y_D=\frac{w_{fD}}{2}} \quad (26)$$

The solution of Equation (32) subjected to the conditions established by Equations (33) and (34) can be solved and the wellbore pressure can be obtained as:

$$\bar{\psi}_{wD} - \frac{1}{2M_{12}}\int_0^1 q_{fD}(\alpha, s)\cdot\theta(x_D, \alpha, s)d\alpha = \frac{\pi}{sC_{fD}h_{fD}}\left[x_D - s\int_0^{x_D}\int_0^{v}\bar{q}_{fD}(x_D, s)dx_D dv\right] \quad (27)$$

where,

$$\theta(x_D,\alpha,s)=\mathrm{K}_0\left(|x_D-\alpha|\sqrt{s\eta_{rD}}\right)+ D_0\cdot\mathrm{I}_0\left(|x_D-\alpha|\sqrt{s\eta_{rD}}\right) +\frac{4}{\pi h_{fD}}\sum_{n=1}^{+\infty}\left[\begin{array}{l}\mathrm{K}_0\left(|x_D-\alpha|\sqrt{s_n}\right)\\ +D_n\cdot\mathrm{I}_0\left(|x_D-\alpha|\sqrt{s_n}\right)\end{array}\right] \cos(n\pi z_D)\cdot\cos(n\pi h_{fzmD})\cdot\sin(n\pi\frac{h_{fD}}{2}) \quad (28)$$

Now, Equation (36) can be numerically solved. If the fracture length is divided into *N* segments (Figure-2) and the flux in each element is assumed to be constant, then we can have:

$$\int_0^1 q_{fD}(\alpha,s)\cdot\theta(x_D,\alpha,s)\mathrm{d}\alpha = \sum_{i=1}^{N}\int_{x_{Di}}^{x_{Di+1}} q_{fDi}(\alpha,s)\cdot\theta(x_{Dj},\alpha,s)\mathrm{d}\alpha \quad (29)$$

where *xDj* is the midpoint of the observation segment.

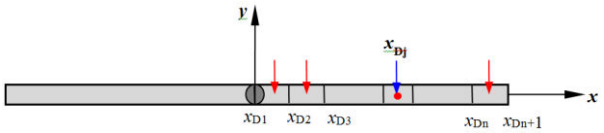

Figure-2. Sketch of the half-fracture discrete element.

The second integral in *Equation* 37 is a Fredholm function, which can be directly solved with the boundary element method, which was presented by Cinco-Ley and Meng (1988):

$$\int_0^{x_D}\int_0^{\nu}\bar{q}_{fD}(x_D,s)\mathrm{d}x_D\mathrm{d}\nu = \sum_{i=1}^{j-1}\bar{q}_{fDi}(s)(j-i)\Delta x_D^2+\bar{q}_{fDj}(s)\frac{\Delta x_D^2}{8} \quad (30)$$

In addition to the above expressions, by considering steady-state flow, we have

$$\Delta x_D\sum_{i=1}^{N}\bar{q}_{fDi}(s)=\frac{1}{s} \quad (31)$$

Equations 25-31 constitute the system of equations that need to be solved for obtaining the unknowns $\bar{q}_{fDi}$ (i=1, 2…N) and $\bar{\psi}_{wD}$.

2.3 Constant-bottom hole-pressure case

When the fractured well produced at a constant pressure, the solution in Laplace space to the well can be expressed by:

$$\bar{q}_D=\frac{1}{s^2\bar{\psi}_{wD}} \quad (32)$$

And the definition of the dimensionless production rate is:

$$q_D=\frac{3.684\times10^{-3}p_{sc}q_{sc}T}{k_{r2}hT_{sc}(\psi_i-\psi_{wf})} \quad (33)$$

2.4 Wellbore storage and skin effects

When the effects of wellbore storage as skin factor are taken into account, the dimensionless wellbore pressure in Laplace space is changed by using the Duhamel's theorem, van Everdingen and Hurst (1949) as follows:

$$\bar{\psi}_{wD}=\frac{s\bar{\psi}_{wDN}+S_{kin}}{s+C_Ds^2\left(s\bar{\psi}_{wDN}+S_{kin}\right)} \quad (34)$$

Being C_D the dimensionless wellbore storage coefficient, $C_D=\frac{C}{2\pi\phi_2c_{t2}hx_f^2}$

3. TRANSIENT-PRESSURE AND RATE-TRANSIENT BEHAVIORS

The dimensionless bottomhole pseudopressure (ψ_{wD}) and pseudopressure derivative ($\mathrm{d}\psi_{wD}/\mathrm{d}t_{Da}$) can be obtained using the Stehfest algorithm, Stehfest (1970) to convert the $\bar{\psi}_{wD}$ back into ψ_{wD}. So, the standard log-log type curves of well test analysis of ψ_{wD} and $w_D'\cdot t_{Da}$ / C_D versus t_{Da} / C_D are obtained.

The standard log-log type curves for rate-transient analysis or rate-decline analysis. Blasingame, McCray, and Lee (1991), Blasingame and Lee (1994), Marhaendrajana, and Blasingame (2001) and Pratikno, Rushing, and Blasingame (2003), can be obtained by defining the following expressions:

Dimensionless decline time

$$t_{Dd}=\frac{t_{Da}}{0.5\left(r_{eD}^2-1\right)\left[\ln\left(r_{eD}\right)-0.5\right]} \quad (35)$$

Dimensionless decline rate function

$$q_{Dd}=q_D\left[\ln(r_{eD})-0.5\right] \quad (36)$$

Dimensionless decline rate integral

$$q_{Ddi}=\frac{\int_0^{t_{Da}}q_{Dd}(\tau)\mathrm{d}\tau}{t_{Da}} \quad (37)$$

Dimensionless decline rate integral derivative

$$q'_{Ddi}=-\frac{\mathrm{d}q_{Ddi}}{\mathrm{d}\ln(t_{Da})} \quad (38)$$

The data provided in Table-1 are used to obtain both the pressure response and the rate decline of the mathematical model derived in this work.

Table-1. Synthetic data used for the discussion of the results.

Parameter	Value
Formation thickness, h , m	100
Wellbore radius, r_w , m	0.1
Fracture height, h_f ,m	50
The radius of inner region, r_m	250
Bottomhole pressure, pwf, MP_a	25
Gas viscosity, μ, cp	0.02
Skin factor, skin	0.1
Inner region	
Horizontal permeability, k_{r1}, mD	10
Vertical permeability, k_{z1}, mD	0.5
porosity, $\emptyset_1$	0.1
Total compressibility, C_t , MP_a^{-1}	1.0E-04
Initial reservoir pressure, p_i, MP_a	30
Half-fracture length, x_f, m	50
The height of the mid-point of the fracture, *hfz*, m	50
Reservoir temperature, T, K	353
Fracture permeability, k_f, D	200
Molecular weight, M_g, kg/mol	16
Wellbore storage coefficient, C , m^3/MPa	0.001
Outer region	
Horizontal permeability, k_{r2}, mD	5
Vertical permeability, k_{z2}, mD	0.25
porosity, $\emptyset_2$	0.2
Total compressibility, C_2 , MPa-1	2.0E-04

It is well known that there are five main flow periods taken place during a transient test of a finite-conductivity fractured well: fracture linear flow, bilinear flow period, formation linear flow period, pseudo-radial flow period and the boundary dominated flow period, Cinco-Ley and Samaniego (1981). For both partially and fully penetrated fractured wells in a composite homogeneous system, the following flow periods can be observed as seen in Figure-3. (1) Fracture linear flow period (see label 1 in Figure-3). This behavior occurs at very small values of dimensionless time, and it can be masked by wellbore storage and skin effects. During this flow period, most of the fluid entering the wellbore comes from the expansion of the fluid in the fracture. The ψ_{wD} and $\psi'_{wD}*t_D$ vs. t_D on log-log curves both for fully and partially fractured well yields a straight line with a slope of one half. (2) Bilinear flow period (see label 2 in Figure-3). The pressure behavior for this flow period exhibits a straight line which slope is equal to one fourth and the duration of this flow period depends on C_{fD}. (3) Formation linear flow period (see label 3 in Figure-3). This flow period is characterized by a half slope in both pseudo pressure and pseudo pressure derivatives curves on log-log scale. (4) Spherical flow period or the pseudo radial flow period in the inner region (see label 4 in Figure-3). For fully penetrated fractured well, the pseudo pressure derivative curve is characterized by a horizontal straight line with the value of "$1/(2*M_{12})$". The duration of this flow period is mainly determined by the inner region radius; for partially fractured well, which is characterized by a negative one-half slope line, and the pseudo radial flow in inner region always be masked by this period. (5) Transition period between inner region and outer region radial flow period (see label 5 in Figure-3). (6) Radial flow period in the outer region (see label 6 in Figure-3). For all the dimensionless parameters defined by the outer region characteristics, the derivative curve of this flow period is characterized by a horizontal well with the value of one half but not "$1/2*M_{12}$". (7) Boundary effect flow period. When the lateral boundary is infinite, this period will not exit. For closed or constant-pressure boundary reservoir, rapid up- or down- curving can be seen on the type curves (see label 7 in Figure-3).

Figures-3 and 4 also show the effects of penetrating ratio (h_{fD}) on type curves of pressure and rate transients. As it can be seen from Figure-3, h_{fD} mainly affects the early flow period in the inner region. When the well produces at a constant flow rate, the smaller h_{fD} the bigger the pressure drop and longer duration of spherical flow period，which reflects a much lower position on the pseudo pressure and its derivative curves. And, when the well produces at a constant bottom hole pressure, high values of h_{fD} represents a large contact face and volume of well with the formation, so no matter what the outer boundary conditions are, the bigger h_{fD} will results into a larger production rate. So, we should obtain fully penetrated fractures as far as possible for the upper and lower boundaries closed reservoir.

Figures-5 and 6 present the effect of the mobility ratio (M_{12}) on the transient pressure and transient rate behavior, respectively. The mobility ratio is defined as the ratio of the inner- region mobility to the outer-region mobility which presents the flow capability of the inner region to the outer. High values of M_{12} allow to recognize that either the micro-fractures around the well are induced or an acidizing stimulation treatment has been conducted. On the contrary, small values of M_{12} can occur by the damage of fracturing fluid or the gas field water re-injected into the abandoned fractured well. It can be seen from Figure-5 if the remaining parameters are kept constant, the mobility ratio has a primary effect on the early line flow and the pseudo radial flow periods. The higher the values of M_{12} is, the lower the pressure drop needed for well production at a constant rate. When the pressure transient reaches the outer region, all the curves

with different M_{12} will coincide. For a well producing at a constant bottomhole pressure, high values of M_{12} will result into a large production rate obeying Darcy's law as shown in Figure-6.

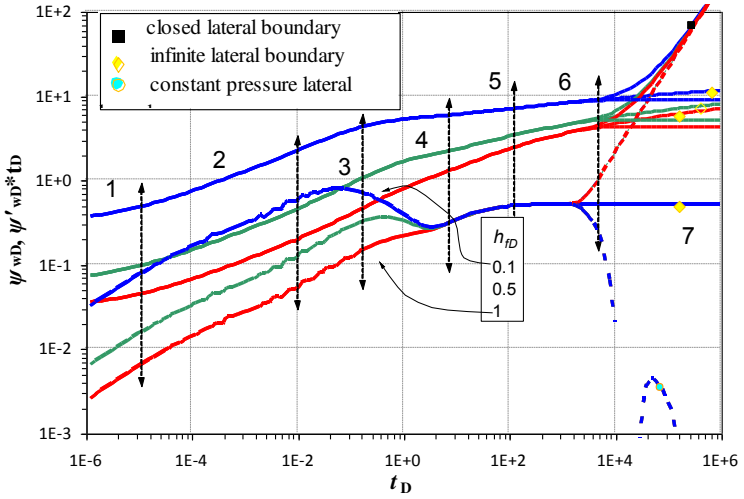

Figure-3. Effect of penetrating ratio (h_{fD}) on the pressure and pressure derivative behaviour.

4. CONSIDERATION A FRACTURE NETWORK INDUCED BY HYDRAULIC FRACTURING

4.1 Model solution

Sometimes, to efficiently develop a low-permeability or an unconventional gas reservoir, massive hydraulic fracturing (MHF) has been widely used around the world which also is a proven technique for developing commercial wells in such formations. The purpose of MHF is to expose a large surface area of the low permeability formation to flow into the wellbore. Massive-scale fracturing fluid and high fluid pressure are the essential requirements for MHF, which activate and connect existing discrete or micro-seismic natural fractures so as to generate large fracture networks. The volume of a reservoir containing the fracture network and the main hydraulic fractures have to be effectively stimulated to increase the well performance. This is referred as Stimulated Reservoir Volume (SRV). In order to describe the SRV in the mathematical model of fractured wells, researchers usually treat the SRV as a dual-porosity system around the well, Ozkan *et al.* (2009, 2011), Chu and Shank (1993), Stalgorov and Mattar (2012a, 2012b) and Apaydin, Ozkan and Raghavan (2012). So, in order to include in this work the pressure and rate transient performance of a MHF well with SRV, the formation is simplified into a composite model with an inner dual-porosity region and an outer homogeneous region with the fractured well centered in the inner region, as depicted in Figure-9.

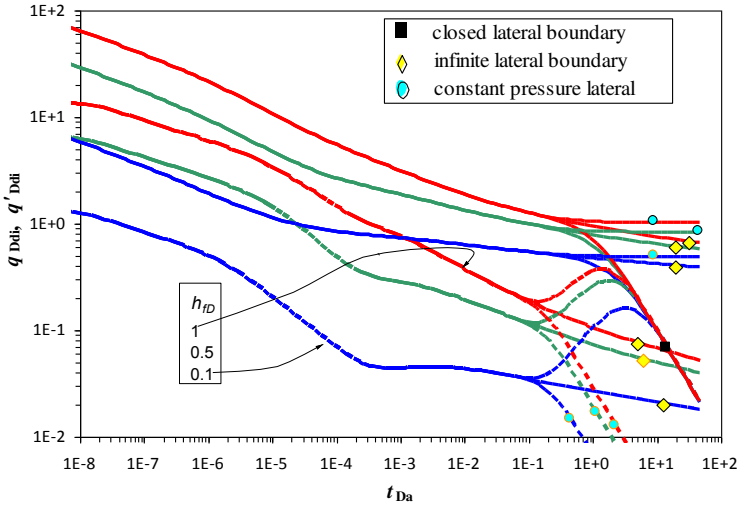

Figure-4. Rate-transient behavior affected by penetrating ratio (h_{fD}).

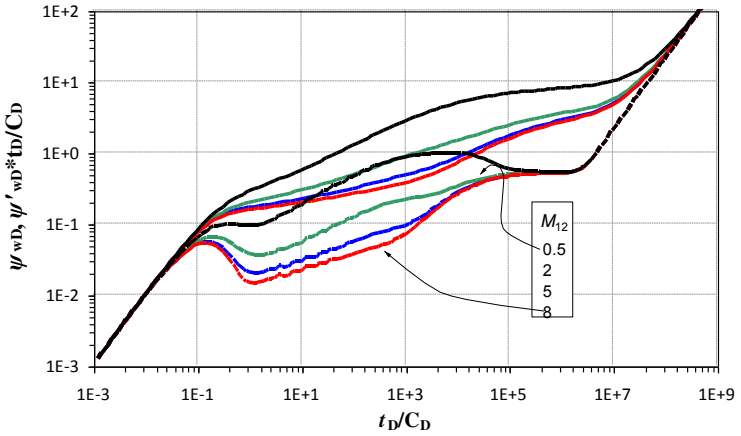

Figure-5. Effects of the mobility ratio (M_{12}) on the pressure and pressure derivative behavior.

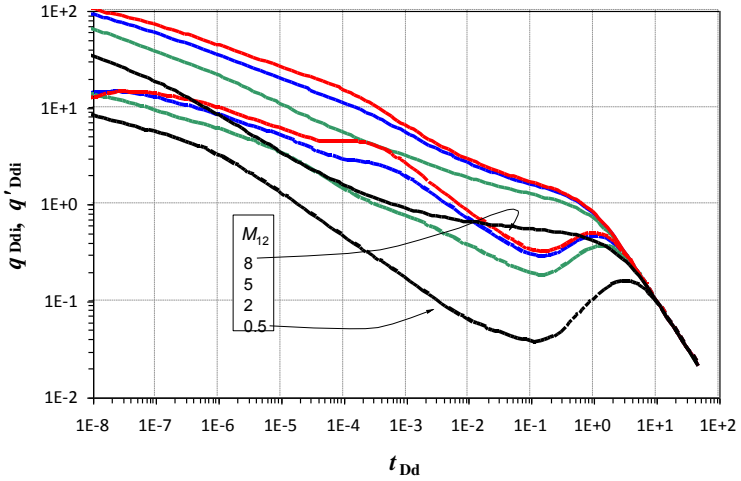

Figure-6. Effects of mobility ratio ($M12$) on the rate-transient behaviour.

Methods for evaluating a conventional (small-volume) fracturing treatment are reported by Prats (1992), Gringarten *et al.* (1974a, 1974b), Cinco-Ley *et al.* (1978), Cinco-Ley and Samaniego (1981) and Mohammed (1993). Using a similar procedure as described in section 2, the continuous point-source function allows obtaining a gas reservoir model with the inner dual-porosity and outer homogeneous regions, comparing to the homogeneous composite model, the only needed change in this model is to substitute the $s\eta_{rD}$ with $s{\cdot}f_1(s)$, and the expression of $f_1(s)$. The corresponding dimensionless variables are given as follows:

$$f_1(s)=\frac{\lambda_{1m\text{-}f}+s\omega_{1f}(1-\omega_{1f})\eta_{rD}}{\lambda_{1m\text{-}f}+s(1-\omega_{1f})\eta_{rD}}\eta_{rD} \tag{39}$$

Where,

$$\omega_{1f}=\frac{(\phi_1 c_{t1})_f}{(\phi_1 c_{t1})_{f+m}} \tag{40}$$

$$\lambda_{1m\text{-}f}=\alpha_1\frac{k_{1m}}{k_{1f}}{x_f}^2 \tag{41}$$

Figures-10 and 11 show the pressure and rate transient responses for different values of storativity ratio of the fracture system (ω_{1f}). The ω_{1f} represents the relative capacity of fluid stored in the fracture system. If ω_{1f} is large, there could be relatively more reserves produced from the fracture system before the interporosity flow period. So that, the pressure drop at early time will be smaller and the trough in the transition flow period will be deeper when the well produces at a constant rate as described in Figure-10. For a well producing at a constant bottom hole pressure, the higher ω_{1f} the higher the dimensionless rate q_{Dd}, but the curves will coincide when reaching the pseudo radial flow period.

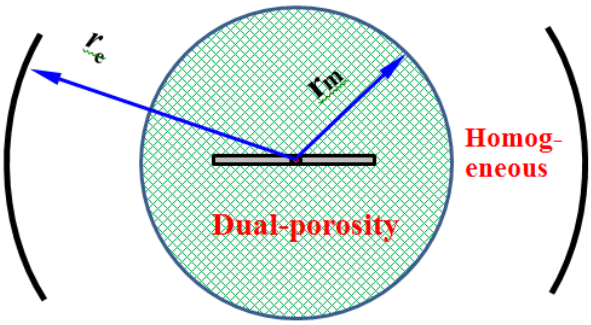

Figure-7. Fractured well with the consideration of fracture network.

4.2. Pressure- and rate-transient behaviours

The data listed in Table-2 are used to analyze the performance of a fractured well with the consideration of stimulated reservoir volume induced by hydraulic fracturing, and the remaining parameters are similar to the composite model provided in Table-1.

Table-2. Synthetic data used for the discussion of the results.

Parameter	Value
Fracture height, h_f, m	100
Half fracture length, x_f, m	30
Inner region	
Fracture system permeability, k_{f1}, mD	50
Interporosity coefficient, $\boldsymbol{\lambda}_{1m\text{-}f}$	1
Matrix system permeability, k_{m1}, mD	5
Storativity ratio, $\boldsymbol{\omega}_{1f}$	0.08

Figure-12 shows the pressure-transient behavior due to the effect of varying the interporosity coefficient ($\boldsymbol{\lambda}_{1m\text{-}f}$). As shown in this plot, as $\boldsymbol{\lambda}_{1m\text{-}f}$ decreases, the interporosity transition flow from matrix to fracture system is delayed. This is due to the fact that the fractures will have to drain more time before the contribution from the matrix becomes significant with larger fracture permeability. When the well produces at a constant bottom hole pressure, the production rate at early time will be larger since more fluid stored in the matrix system is extracted as described in Figure-13.

5. CONCLUSIONS

a) Mathematical models to describe both pressure- and rate-transient responses for a vertical well having a finite-conductivity fracture with either full or partial penetration within a system with different lateral boundaries is introduced. Pressure- and rate-transient behaviours under different sensitive parameters or scenarios are analyzed.

b) Application of the point-source function and Laplace transformation are used to provide both the pressure and rate transient solutions for a well with partially and fully penetrated well in a composite gas reservoir. Also, a new composite model considering inner dual-porosity medium to describe the stimulated reservoir volume around the well is proposed and solved.

c) Comparing the fractured-well pressure response obtained from partially and fully penetrated fractures, the following flow regimes are observed: fracture linear, bilinear, formation linear, spherical -for partially penetrated- and pseudo radial, transition, pseudo radial in the outer region and boundary reflection flow periods.

d) The permeability and radius of the inner region have a major effect on well productivity when the well is operated under a constant-bottom hole pressure, so in such cases, formation damage is minimized and the generation of a fracture network is likely to take place during the fracturing process.

e) For the development of tight and unconventional gas reservoirs, massive hydraulic fracturing is a necessary technology to be implemented. The fracturing process mitigates formation damage and induces the development of a quality fracture network which leads to the stimulation of some reservoir volume.

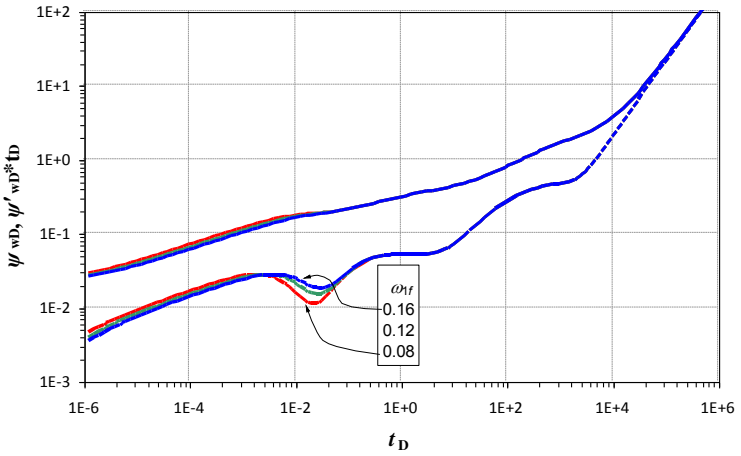

Figure-8. Effect of the storability ratio (ω_{1f}) on the pressure behavior of a well with a fracture network collaterally created by the fracturing treatment.

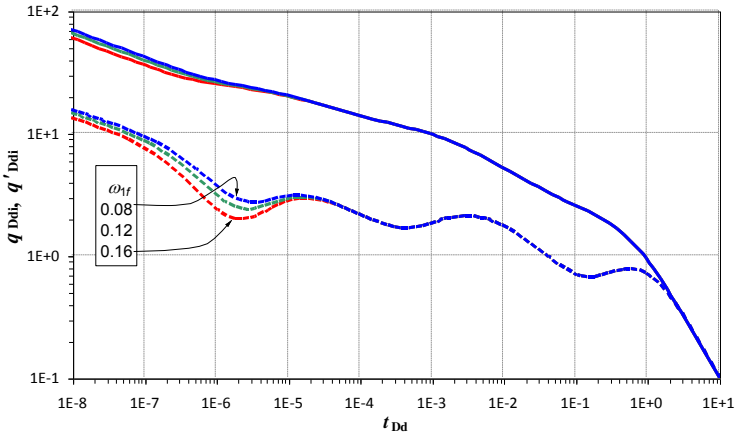

Figure-9. Effect of the storability ratio (ω_{1f}) on the rate behavior of a well with a fracture network collaterally created by the fracturing treatment.

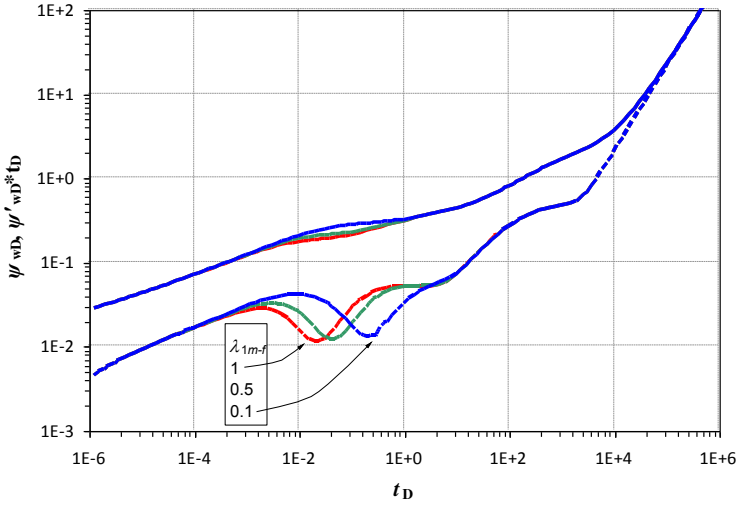

Figure-10. Effect of the interporosity flow coefficient ($\lambda_{1m\text{-}f}$) on well pressure behavior considering a fracture network.

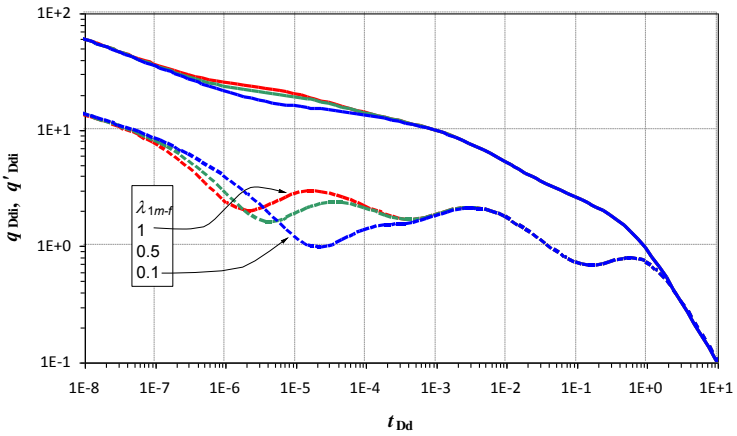

Figure-11. Effect of the interporosity flow coefficient ($\lambda_{1m\text{-}f}$) on rate-transient response including a fracture network presence.

ACKNOWLEDGEMENT

This work was supported by Scientific Research Starting Project of SWPU (No. 2015QHZ003). The authors would also like to appreciate the reviewers and editors whose critical comments were very helpful in preparing this article.

Nomenclature

c_{t1}, c_{t2}	total system compressibility, MP_a^{-1}
C	wellbore storage coefficient, m3/MPa
h	formation thickness, m
h_f	fracture height, m
h_{fzm}	distance from the fracture middle point to the reservoir's bottom boundary, m
$I_0(x)$, $K_0(x)$	modified Bessel function of first and second kind respectively, zero order
$I'_0(x)$, $K'_0(x)$	modified Bessel function derivative of first and second kind respectively, zero order
k_1, k_2	effective permeability of regions 1 and 2, D
k_{r1}, k_{r2}	horizontal permeability of regions 1 and 2, D
k_{z1}, k_{z2}	vertical permeability of regions 1 and 2, D
k_f	fracture permeability, D
M_{12}	mobility ratio between regions 1 and 2
p_{sc}	pressure at standard state condition, p_{sc} 0.10325 MPa
p	pressure, MPa
p_f	pressure in hydraulic fracture, MPa
q_{sc}	gas flow rate at standard condition, m3/d
q	continuous point source withdraw rate, m/d
q_{Dd}	dimensionless decline rate function, defined in Eq.(45)
q_{Ddi}	dimensionless decline rate integral, defined in Eq.(46)
q'_{Ddi}	dimensionless decline rate integral derivative, defined in Eq.(47)
r_m	discontinuity radius for region 1, m
r_w	well radius, m
s	Laplace variable
S_{kin}	skin factor
T	temperature at reservoir state condition, K
T_{sc}	temperature at standard state condition, T_{sc}=293K
t	production time, h
$t_a(p)$	pseudo-time function, MPa*h/cp
t_{Dd}	dimensionless decline rate, defined in Eq.(44)
w_f	fracture width, m
W_{12}	storativity ratio between region 1 and 2
x, y, z	distance in the Cartesian coordinate system, m
x_f	fracture half length, m
Z	gas deviation factor, sm^3/m^3
η_{12}	diffusivity ratio between regions 1 and 2
$\omega_{1m\text{-}f}$	storability ratio of fracture system for fracture network model
$\lambda_{1m\text{-}f}$	interporosity coefficient from matrix system to fracture system for fracture network model
μ	gas viscosity, cp
$\emptyset_1$,$\emptyset_2$	porosity of region 1 and region 2

REFERENCES

[1] Ahmed U. 1982. Transient pressure analysis of hydraulically fractured wells in the Western tight sands. SPE 10878 presented at SPE Rocky Mountain Regional Meeting, 19-12 May, Billing, Montana.

[2] Apaydin O.G., Ozkan E. and Raghavan R. 2012. Effect of discontinuous microfractures on ultratight matrix permeability of a dual-porosity medium. SPE Reservoir Evaluation and Engineering. 15(4): 473-485.

[3] Agarwal G. 1979. Real gas pseudo-time a new function for pressure buildup analysis of MHF gas wells. Paper SPE 8279 presented at the 54th technical conference and exhibition of the Society of Petroleum Engineers of AIME, Sep. 23-26, Las Vegas, NV.

[4] Blasingame T.A., Mccray T.L. and Lee W.J. 1991. Decline curve analysis for variable pressure drop/variable flow rate systems. Paper SPE-21513-

MS presented at SPE Gas Technology Symposium, 22–24 January, Houston, Texas.

[5] Blasingame T.A. and Lee W.J. 1994. The variable-rate reservoir limits testing of gas wells. Paper SPE 17708-MS presented at SPE Gas Technology Symposium, 13-15 June, Dallas, Texas.

[6] Brown M., Ozkan E. and Raghavan R. 2011. Practical solutions for pressure-transient responses of fractured horizontal wells in unconventional reservoirs. SPE Reservoir Evaluation and Engineering. 14(6): 663-676.

[7] Chu W.C. and Shank G.D. 1993. A new model for a fractured well in a radial, composite reservoir (includes associated papers 27919, 28665 and 29212) SPE Formation Evaluation. 8(3): 225-232.

[8] Chen C.C. and Raghavan R. 1995. Modeling a fractured well in a composite reservoir. SPE Formation Evaluation, 10(4): 241-246.

[9] Cinco-Ley H. and Samaniego V., F. 1977, January 1. Effect of Wellbore Storage and Damage on the Transient Pressure Behavior of Vertically Fractured Wells. Society of Petroleum Engineers. doi:10.2118/6752-MS.

[10] Cinco-Ley H. and Samaniego F. 1981. Transient pressure analysis for fractured wells. Journal of Petroleum Technology. 33(9): 1749-1766.

[11] Cinco-Ley H., Samaniego F. and Dominguez N. 1978. Transient pressure behavior for a well with a finite-conductivity vertical fracture. SPE Journal. 18(4):.253-264.

[12] Cinco-Ley H., Samaniego F., Rodriguez F. 1989. Application of the pseudolinear-flow model to the pressure-transient analysis of fractured wells. SPE Formation Evaluation. 4(3): 438-444.

[13] Cinco-Ley H. and Meng H. Z. 1988, January 1. Pressure Transient Analysis of Wells with Finite Conductivity Vertical Fractures in Double Porosity Reservoirs. Society of Petroleum Engineers. doi:10.2118/18172-MS.

[14] Escobar F.H., Zhao Y.L. and Zhang L.H. 2014. Interpretation of Pressure Tests in Hydraulically-Fractured Wells in Bi-Zonal Gas Reservoirs. Ingeniería e Investigación. ISSN 0120-5609. Vol. 34. Nro. 4. pp. 76-84. 2014.

[15] Feng J.D., Luo R.L. and Chen L.S. 2009. A composite seepage model for fractured reservoir. Paper SPE119255 presented at SPE Annual Technical Conference and Exhibition, 15-18 March, Bahrain.

[16] Fjaer E. 2008. Mechanics of hydraulic fracturing. Petroleum related rock mechanics. Developments in petroleum science (2nd Ed.). Elsevier. pp. 369. Retrieved 2012-05-14.

[17] Gringarten A.C., Ramey Jr., H.J., Raghavan R. 1974a. Unsteady state pressure distribution created by a well with a single infinite conductivity vertical fracture. SPE Journal. 347-360 (August).

[18] Gringarten A.C., Ramey Jr., H.J., Raghavan R. 1974b. Unsteady state pressure distribution created by a well with a single infinite conductivity vertical fracture. SPE Journal. 14(4): 347-360.

[19] Hanley E.J. and Bandyopadhyay P. 1979. Pressure transient behavior of the uniform flux finite capacity fracture. SPE 8278 presented at the SPE Annual Technical Conference and Exhibition, 23-26 September, Las Vegas, Nevada.

[20] Marhaendrajana T. and Blasingame T.A. 2001. Decline curve analysis using type curves-evaluation of well performance behavior in a multiwell reservoir system. Paper SPE-71517-MS presented at SPE Annual Technical Conf. and Exhibition, 30 September-3 October 2001, New Orleans, LA.

[21] Mohammed E.O. and Kassem J.H.A. 1997. A new method for pressure test analysis of a vertically fractured well producing commingled zones in bounded square reservoirs. Journal of Petroleum Science and Engineering. 18(1-2): 131-145.

[22] Mohammed E.O. 1993. Pressure analysis of a fractured well in multilayered reservoirs. Journal of Petroleum Science and Engineering. 9(1): 49-66.

[23] Ozkan E., Brown M., Raghavan R. and Kasemi H. 2009. Comparison of fractured horizontal-well performance in conventional and unconventional reservoirs. SPE 121290-MS presented at SPE Western Regional Meeting, San Jose, California, 24-16 March.

[24] Ozkan E., Brown M., Raghavan R. and Kasemi H. 2011. Comparison of Fractured-Horizontal-Well Performance in Tight Sand and Shale Reservoirs. SPE Reservoir Evaluation and Engineering. 14(2): 248-259.

[25] Prats M. 1961. Effect of vertical fractures on reservoir behavior-incompressible fluid case. Society of Petroleum Engineering Journal. 1(2): 105-118.

[26] Pratikno H., Rushing J.A. and Blasingame T.A. 2003. Decline curve analysis using type curves-fractured wells. SPE 84278-MS presented at SPE Annual Technical Conference and Exhibition, 5-8 October, Denver, Colorado.

[27] Stalgorova E. and Mattar L. 2012a. Practical Analytical model to simulate production of horizontal wells with branch fractures. SPE 162515 presented at SPE Canadian Unconventional Resource Conference, 30 Oct.-1 Nov, Calgary, Alberta, Canada.

[28] Stalgorova E. and Mattar L. 2012b. Analytical model for history matching and forecasting production in multifrac composite systems. SPE 162516-MS presented at SPE Canadian Unconventional Resource Conference, 30 October.-1 November, Calgary, Alberta, Canada.

[29] Stehfest H. 1970. Numerical inversion of Laplace transform, Communication ACM. 13: 47-49.

[30] Van Everdingen V. and Hurst A.F. 1949. The application of the Laplace transformation to flow problem in reservoirs. Journal of Petroleum Technology. 1(12): 305-327.

[31] Zhao Y.L. 2011. The theory and application of source functions in bi-zonal gas reservoirs. MSc. Thesis. Southwest Petroleum University. China. (In: Chinese).

[32] Zhao Y.L., Zhang L.H., Hu S.Y., Zhao J.Z. and Zhang B.N. 2013. Transient pressure analysis of fractured well in bi-zonal gas reservoirs. Journal of Hydrology. 524: 89-99.